

Deformation Analysis of Composite Reinforcing Fabrics through Yarn Pull-out, Drape and Shear Tests

Bidour Al-Gaadi*, Marianna Halász

Budapest University of Technology and Economics, Faculty of Mechanical Engineering,
Department of Polymer Engineering, Budapest H-1111, Hungary

Abstract

This study reveals a new method based on image processing of bias extension test results to determine shear angle that characterizes the shear properties of fabric reinforcements. This way the simple and exact determination of shear angle with conventional devices is solved. The new method was tested on fabric reinforcements made of carbon, aramid and glass fibers and the results were compared with that of two known versions of bias extension tests. The analysis of the relation between shear angle and other deformation properties that characterize spatial deformation behavior involved the comparison of shear test results with yarn pull-out and drape tests carried out with special methods.

Key words: fabric reinforcement, drapability, shear angle, bias extension, yarn pull-out

1. Introduction

Woven structures are often applied in composite products as reinforcement, due to their complex deformation behavior and excellent mechanical properties. When covering a spatial, complex surface or preparing a complex 3D product, the fabric is subjected to shearing (in its plane) and bending (perpendicular to its plane) stress, and meanwhile draping occurs. Much research is carried out on the examination and modeling of this special deformation process [1-6], but this field is still not revealed completely. The mechanical examination of the fabric reinforcements cannot

always be completed with the conventional textile test methods and devices, because the properties are so different that the measurement limits of the conventional devices are exceeded. Therefore, the examination of these fabrics requires the overview and improvement of old methods and also the development of new methods. Image processing makes it possible to develop such new methods, the advantages of which are applied more and more widely, especially in case of the examination of deformation processes [7-9].

Spatial deformation behavior of fabrics can be characterized by the results of drape tests in an integrated way [10-13]. The tensile, bending and shear properties of fabrics that influence its drapability to the greatest extent can also be measured separately, and based on that complex deformation behavior can be estimated. The shear properties of fabrics are strongly connected to the interactions among the yarns that make up the fabric. A frequent test method of the complex interactions among the yarns, mainly the friction forces among them is the so called yarn pull-out test [14-16].

There are three widespread methods for the determination of the shear properties of fabrics [17-20]: examination with Kawabata (KES-F) equipment, picture frame and bias extension tests. In case of the Kawabata shear test the sample has to be clamped on its two opposite sides – similarly to tensile tests – and the clamp moving parallel with the standing one exerts shearing stress. However, the KES-F device can measure maximum 8° shear angle of conventional textiles. In case of picture frame tensile tests the sample is clamped into a quadratic frame that is connected by joints in the corners, then the frame is pulled diagonally with a tensile tester device. During bias extension shear force and shear deformation is determined from the tensile test of the sample cut from the fabric in a $\pm 45^\circ$ angle compared to the weft direction. Bias extension can be carried out with a SiroFAST (Fabric Assurance by Simple Testing) device or a tensile tester, however the FAST equipment – like the KES-F device – is prepared primarily for the examination of conventional textiles.

Potluri et al [18] compared the three shear examination methods. They found that the disadvantage of picture frame tensile tests is that no pure shear is present along the clamping and clamping problems may also arise. It was concluded that shear stress values obtained from bias extension method coincide with the values measured on the KES device well.

Lomov et al [21] concluded that the advantage of bias extension compared to the picture frame method is its simplicity and that the yarn ends are free in the pure shear zone, therefore the process is closer to reality. The only disadvantage of bias extension is that inaccuracy may arise due to image processing.

Harrison et al [22] carried out both picture frame and bias extension tests. They concluded that the deformation process that occurred during the picture frame test is closer to the process that takes place during the production of composite parts compared to bias extension. However, bias extension provides faster and more reliable results on the angle between the yarns of the fabric compared to the picture frame method, due to the opposite effects caused by the criteria of the picture frame method

The aim of this study is to develop a new version of bias extension examination based on image processing that makes it possible to determine the shear angle in a simple and accurate way using conventional devices. The new method was tested on reinforcing fabrics made up of carbon, aramid and glass fibers, and the results were compared to two known versions of bias extension. In order to analyze the relation between shear angle and other deformation properties characterizing spatial deformation behavior the results of shear tests were compared to that of yarn pull-out and drape tests carried out with special methods.

2. Bias extension method

This chapter presents the principle of bias extension tests and the methods of shear angle determination. Our review of literature in this field revealed two main methods for the determination of shear angles: one that is based on geometry applied by Lebrun and the image

processing method applied by Domskienė and Strazdienė. The method developed by us was compared to these two methods.

2.1 Principle of bias extension tests

During bias extension shear force and shear deformation are determined from the tensile tests of the sample cut from the fabric in a $\pm 45^\circ$ angle compared to the weft direction. Shear deformation is often characterized by the change in the angle of the fabric yarns, and is called shear angle, usually denoted by γ (Figure 1).

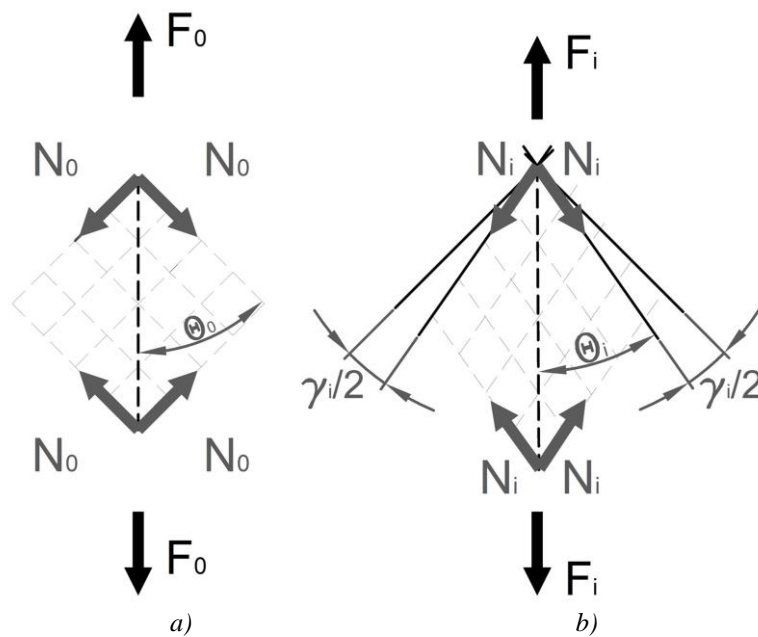


Figure 1 Shear angle change due to loading

a) Angle of the warp and weft yarns of the fabric in an unloaded state

b) Shear angle and angle of the warp and weft yarns of the fabric in a loaded state

In case of bias extension the extent of shear in the different parts of the examined sample is not the same. Determination of the shear angle has to be carried out in the range of the sample where pure shear deformation can be found. Shear deformation is pure if there is no slippage when the yarns turn on each other. In case of bias extension the requirement of pure shear deformation needed for the examination is that the initial length-width ratio (λ) of the sample has to be higher than 1 (Figure 3, $\lambda = h_0/w_0$, where h_0 and w_0 are the initial clamped sample length and width,

respectively). If $\lambda \leq 1$, the single yarns are clamped both in the top and bottom clamp and therefore hinder shear deformation during extension. Ratio $\lambda \leq 2$ provides that most of the clamped sample has pure shear stress during the test and there is enough elongation before the failure of the sample [23].

Three zones are created in the examined sample during bias extension. The extent of shearing in the different zones is the following (Figure 2) [18, 21, 23, 24]:

- in zone A, in the middle of the sample pure shear arises,
- in zones C, at the two ends of the sample no shear takes place,
- between the two zones, in zones B half of the shear that is present in zone A arises.

Since pure shear is only present in the middle of the sample, in zone A, the determination of shear angle has to be carried out there.

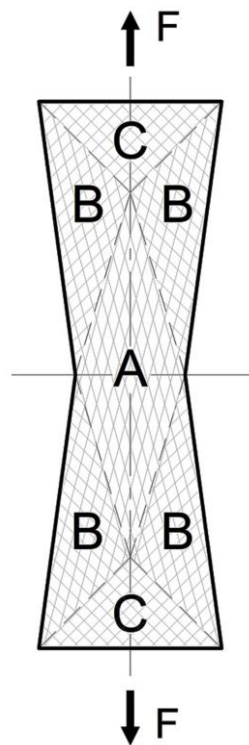


Figure 2 Shear zones during loading [25]

2.2 Shear angle determination based on geometry

Lebrun [25] determined the shear angle in the extended fabric sample using formula (1) for which only the initial geometrical data and actual elongation value of the sample are needed (Figure 3).

$$\gamma_i = 90^\circ - 2\theta_i = 90^\circ - 2\arccos\left(\frac{h_0 + \delta_i}{\sqrt{2}h_0}\right) \quad (1)$$

where θ_i is half of the angle between the warp and weft direction yarns, h_0 is the initial clamped length of the sample, while δ_i is the actual elongation.

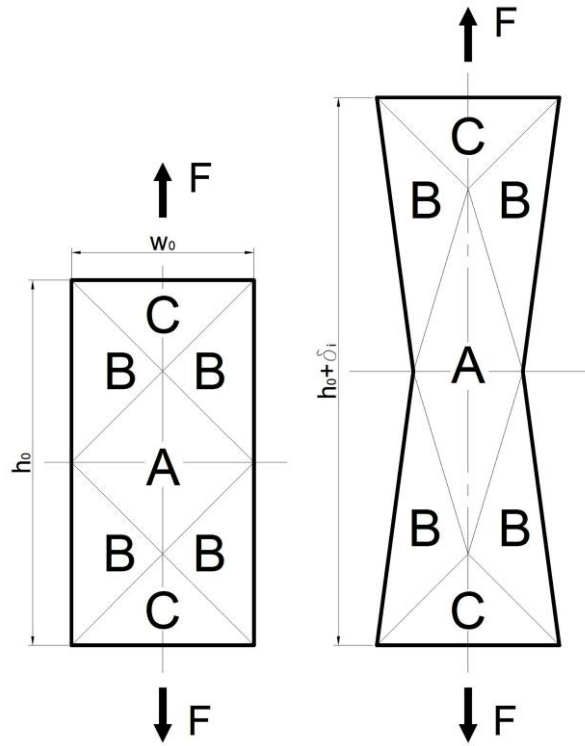


Figure 3 Shear angle determination with bias extension method [25]

2.3 Shear angle determination based on image processing

Domskiené and Strazdiené [10] applied image processing for the determination of shear angle. Before starting the examination Domskiené and Strazdiené draw rhombs, the sides of which are parallel with the yarns of the fabric, as shown in Figure 4. During the examination photographs are taken of the images and an adequate image processing program determines the angle of the sides of the rhomb, i.e. the angle of the fabric yarns directly. Angles θ_i are determined in every single image in the 4 locations shown in Figure 4, and using formula (2) below the shear angle that belongs to the actual stress can be calculated.

$$\gamma_i = \frac{\sum_{k=1}^4 (90^\circ - 2\theta_{ik})}{4} \quad (2)$$

where γ_i is the shear strength that belongs to the actual stress, θ_i is the half of the actual angle of the warp and weft yarns and $k=1, 2, 3, 4$ are the 4 examination points of the sample.

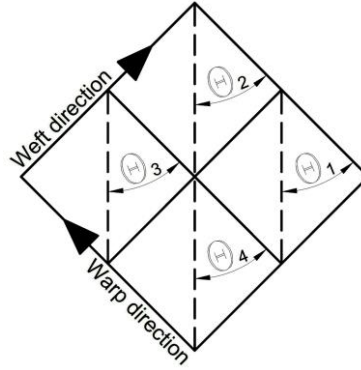


Figure 4 Shear angle determination based on image processing

2.4 Shear force determination

During extension the yarn directional components of the tensile force exert shear stress on the fabric. If the shear angle is known shear force N – the yarn directional component – can be determined from tensile force F (Figure 5). Since the shear force in the direction of the two yarn systems and the angle between the yarns are the same, shear force N [23] that arises in the fabric can be described as a function of the actual angle between the warp and weft yarns and the actual tensile force (3). The actual angle between the warp and weft yarns can be calculated from the actual shear angle using formula (4).

$$N_i = \frac{F_i}{2 \cos \theta_i} [N] \quad (3)$$

$$\theta_i = \frac{2\theta_0 - \gamma_i}{2} \quad (4)$$

where N_i is the average actual shear force, F_i is the actual tensile force, θ_0 is the half of the initial angle of the warp and weft yarns, γ_i is the actual shear angle, θ_i is the half of the actual angle of the warp and weft yarns and i is the given moment (time).

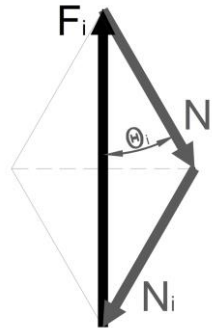


Figure 5 Shear angle in the fabric due to bias extension

3. Novel shear angle determination method

A new method was developed for the evaluation of bias extension tests with the help of which shear angle can be determined in a more simple and accurate way than described above. An important element of the new method is that not only the longitudinal elongation of the examined sample is used for the calculation of the shear angle but also the decrease of cross directional width. The dimensional change of the sample is determined by an image processing method, and for this purpose longitudinal and crosswise lines were drawn on the sample before the examination, as shown in Figure 6.a. The drawn lines create a rectangle in the pure shear zone, and a square in case of an ideal sample. The sample is ideal if the angle of the warp and weft yarns in the fabric is 90° before the test. The lines have to be drawn in a way that the centers of the sides of the rectangle or square shall form a rhomb or in case of an ideal sample a square the sides of which are parallel with the yarns of the fabric. During the examination, the actual distance of these lines at the locations defined in Figure 6.b, i.e. in the longitudinal and crosswise center lines of the sample are recorded. The same result could be achieved if photographs were taken and analyzed later, however this would require much more manual work. The other essential element of the new method is the application of a video extensometer with which the necessary distances can be recorded

continuously and automatically. The video extensometer finds and collects the required distances automatically using the contrast of the sample without the need for recording every single image.

Shear angle can be calculated easily from the longitudinal and crosswise dimensional change of the fabric (Figures 6.a and b) using formula (5). Another novelty of the method is that it can take into consideration if the sample is not ideal, i.e. the initial angle between the warp and weft yarns is not exactly 90° , since this might often be the case due to the deformation of fabrics during production.

$$\gamma_i = 2\theta_0 - 2\theta_i = 2\theta_0 - 2\arctg \frac{a_i}{b_i} \quad (5)$$

where γ_i is the actual shear angle, θ_0 is the half of the initial angle of the warp and weft yarns, θ_i is the half of the actual angle of the warp and weft yarns, a_i is the half of the actual crosswise distance between the drawn lines, and b_i is the half of the actual longitudinal distance between the drawn lines.

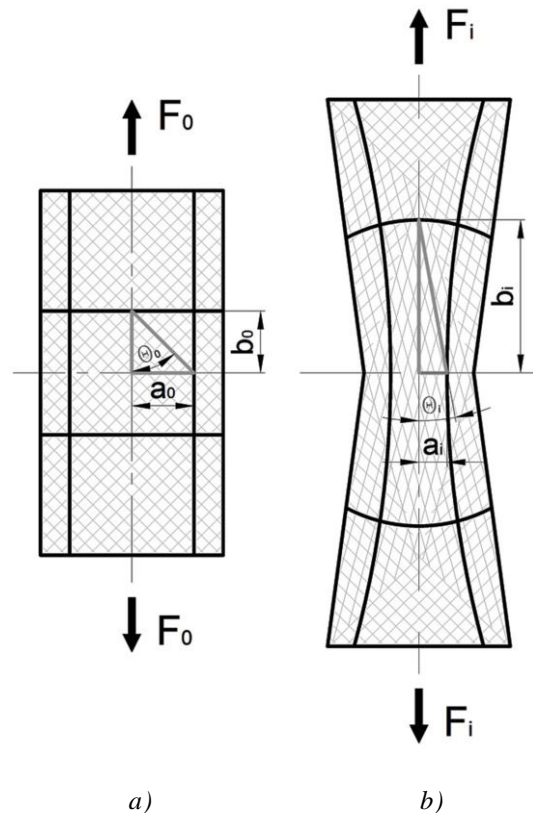


Figure 6 Determination of shear angle γ using a video extensometer

a) Marked sample in unloaded status b) Marked sample in loaded status

4. Experimental

Four different composite reinforcing fabrics (Table 1) were examined and there is no connection between the properties of the fabrics. The weave types are plain and 2/3 twill, which are most often used in composite fabric reinforcements. The base material is glass, carbon and aramid fibers, the most often used base materials of fabric reinforcements (Figure 7).

Table 1 Properties of experimental fabrics

| No. | Material | Weave type | Area density [g/m ²] | Yarn density [1/10 mm] | | Yarn fineness [tex] | |
|-------------|----------|------------|-------------------------------------|---------------------------|------|------------------------|------|
| | | | | Warp | Weft | Warp | Weft |
| G163 | glass | 2/2 twill | 163 | 12 | 12 | 70 | 70 |
| G220 | glass | plain | 220 | 6 | 6 | 220 | 220 |
| K170 | kevlar | 2/2 twill | 170 | 6 | 6 | 130 | 130 |
| C160 | carbon | plain | 160 | 4 | 4 | 200 | 200 |

Since the weave type of all 4 fabrics is symmetric and their warp and weft yarns are identical, it was not necessary to measure separately in warp and weft directions. Special attention has to be paid to the stability of samples during sample preparation since all yarns are quite slippery.

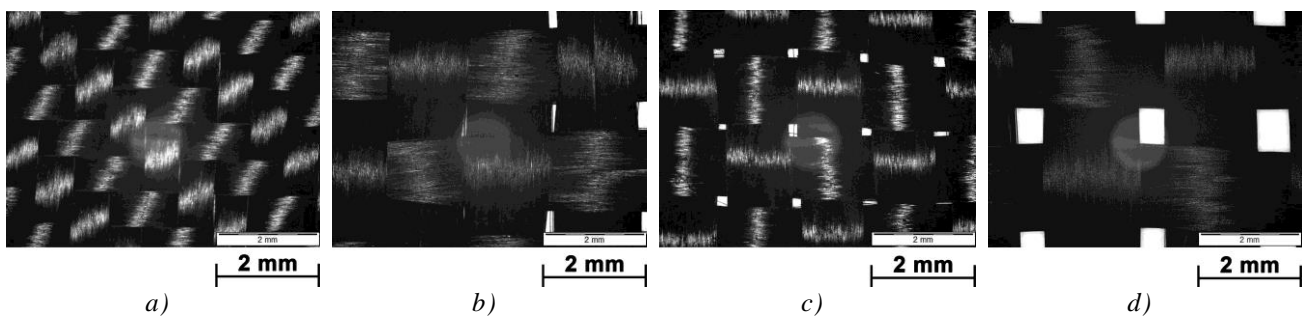


Figure 7 Microscopic recording of woven fabrics

a) G163 b) G220 c) K170 d) C160

4.1 Shear examinations

Bias extension tests were carried out on 50 mm wide and 200 mm long samples, using 100 mm examination length. The samples were cut in 45° compared to the weft direction. Shear angle

was determined using all the three methods in case of every sample in order to be able to compare the results correctly. The lines necessary for image processing were drawn on one side of the samples, while other lines needed for our method were drawn on the other side of them. This way images necessary for image processing could be taken, and meanwhile the data needed for recording with the video extensometer were also available.

Careful marking with adequate contrast is essential considering the accuracy of the measurement, as well as the prevention of the slipping of yarns in the samples during sample preparation and when clamping into a tensile tester. A method similar to the paper frame method used in case of elementary fibers was applied during sample preparation in order to prevent the slipping of the yarns of the fabric [26]. The first step of sample preparation was to mark 5 samples on the fabric, and the figure needed for the image processing method was drawn on them. Then two sides of a 200 mm wide and 250 mm long paper sheet were glued on the marked samples in 50 mm bands in a way that the glued parts were placed on the clamped ends of the sample. The samples were cut out with the glued paper on them, and finally the lines needed for our own developed method were drawn on their other side. The cut out and marked samples were clamped into the tensile tester together with the paper glued on them and before starting the test, the part of the paper between the two clamping jaws was removed.

Shear tests were carried out on a universal, computer controlled tensile tester, type Zwick Z005 with a 5kN force measuring cell, at 10 mm/min tensile rate at room temperature on all materials. During the examination longitudinal elongation and crosswise width decrease were measured continuously by a video extensometer based on the marks drawn on the sample, with simultaneous crosshead movement and tensile force recording. Meanwhile images needed for image processing were taken with a digital camera. Figure 8 illustrates the change of the sample during bias extension.

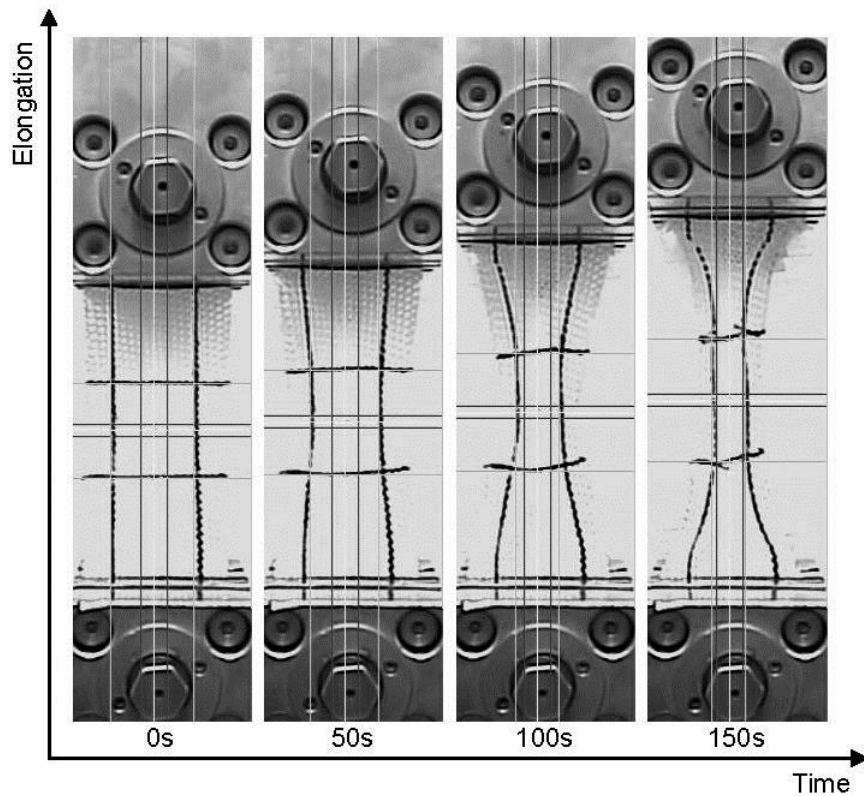


Figure 8 Photographs series taken of the changes during bias extension of the sample

4.2 Yarn pull-out measurements

Yarn pull-out measurements reveal information on the interactions among the yarns of the fabrics, mainly on the friction between yarns. Figure 9 presents the special design and dimensions of the specimens.

Adequate clamping of the sample had to be solved before starting the measurement and undesired slipping of the fabric had to be prevented, as well. Both problems were solved by forming composite parts on the sample. Figure 9 shows the hatched parts that were prepared by manual lamination using glass fiber mats and polyester resins in 50 mm width on the two sides, and on the bottom and the top.

The laminated bottom of the sample is clamped with a general, 60 mm wide clamping jaw, and the yarn to be pulled out is clamped with a yarn clammer on the top, while the laminated bands provide the lateral clamping automatically. The examination was carried out with 10, 20 and 36 crossing yarns. Before starting the measurement the yarn to be pulled out was cut in the bottom

after the given yarn number. Yarn pull-out was done on a Zwick Z005 universal, computer controlled tensile tester with a 20 N force measurement cell at room temperature.

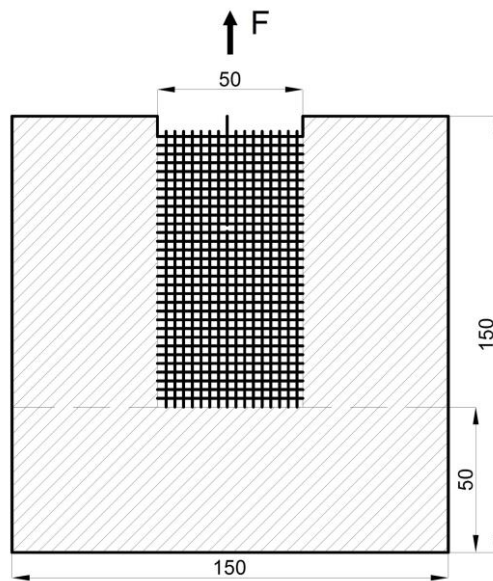


Figure 9 Yarn pull-out measurement

Figure 10 illustrates the set-up of the yarn pull-out measurements.

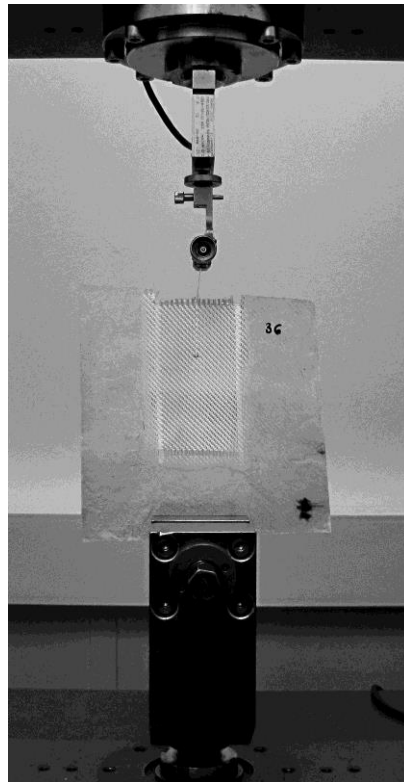


Figure 10 Set-up of the yarn pull-out measurement

4.3 *Drape measurement*

Drability of the samples was measured with the Sylvie 3D Drape Tester (Figure Figure .a) developed at BME. It is a computer controlled measuring device using a 3D scanning technique and image processing [12]. The device raises the 180 mm diameter sample holding table automatically with the 300 mm diameter sample on it at 3.25 mm/s even velocity. After 3D scanning the software of the Sylvie 3D Drape Tester produces the measured surface virtually based on the recorded data, and calculates data characteristic of draping. The device can be used for conventional measurement (according to standard DIN 54306), when drapes form only due to gravitation, but it can be equipped with different diameter rings that influence drape formation dynamically [27].

If draping of fabric reinforcements is measured in the conventional way, the problem that due to the rigidity of the fabric no measureable drapes form on the sample arises. With the help of a special solution, rings that influence the formation of drapes dynamically measurements can be carried out in case of reinforcing fabrics as well and evaluable results can be achieved. The essence of the modified measurement is that the sample holding table raises the sample through the ring before 3D scanning while the ring exerts temporary pressure on the drapes of the sample (Figure 11.b). This temporary pressure keeps the drapes of the sample held down and this way the flexible resistance of the fabric and the sticking friction that prevents the turning of yarns on each other are both overcome and a deformation is triggered dependent on the inner diameter of the ring. After the pressure effect of the ring is stopped, this triggered deformation can get back to its original shape only partly – mainly because the sticking friction among yarns hinders that. Hence the deformation of the sample will be larger and easier to measure than in case drapes are formed only due to gravity. As a result the conditions of the measurements carried out with the ring are closer to reality than in case of conventional measurements without a ring. Several other external effects influence the behavior of the material besides gravity, and these effects are modeled with the ring during the measurement. The ring makes it possible to show the difference between the drape coefficients of difficult-to-drape fabric reinforcements.

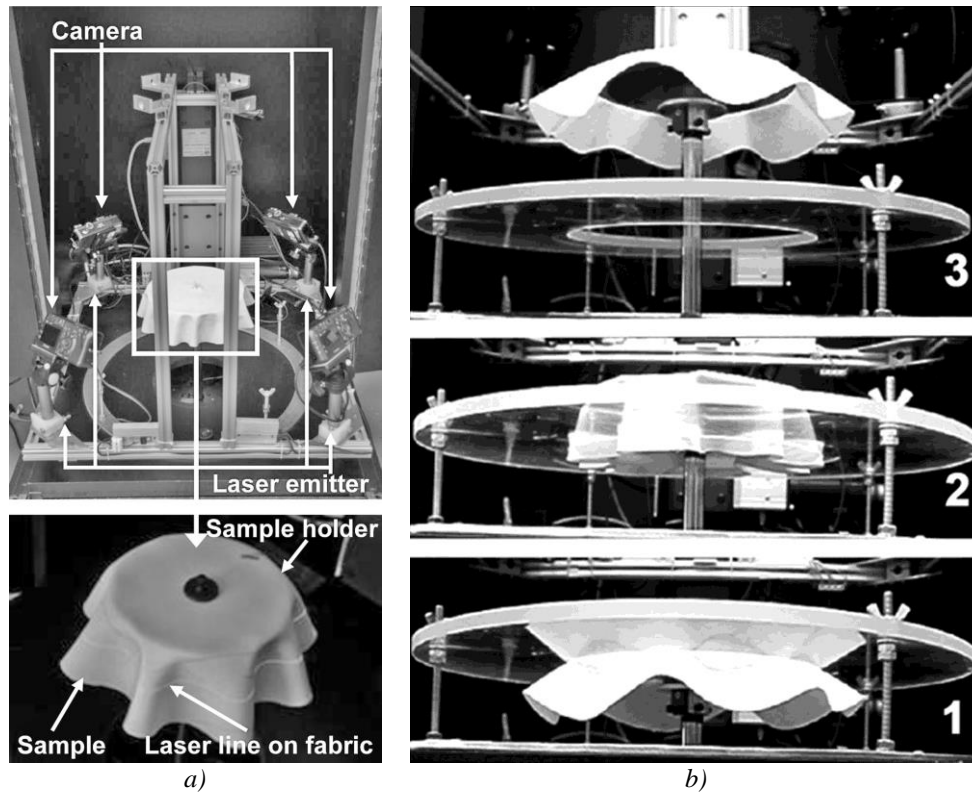


Figure 11 Sylvie 3D Drape Tester

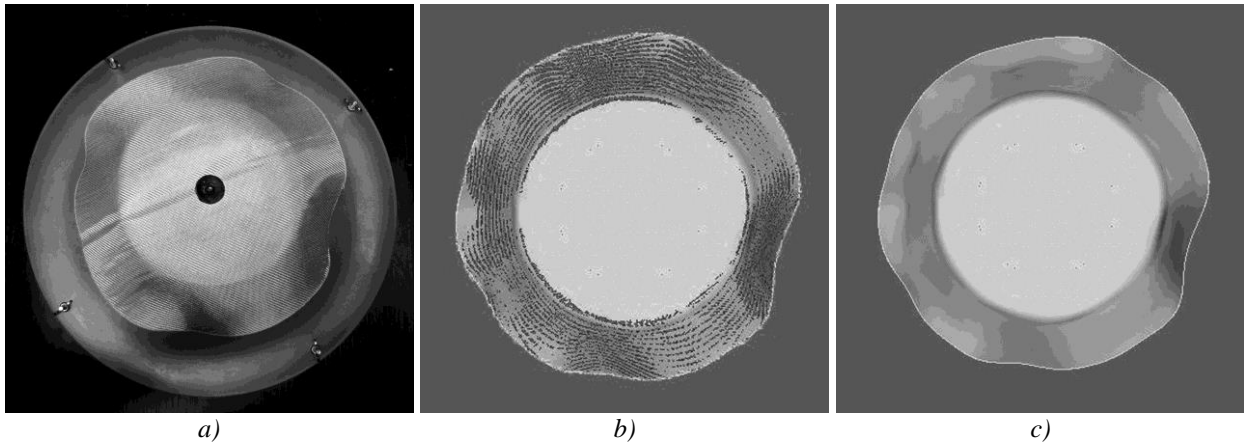
a) Device with the sample b) Examination of the sample using the ring

Draping is measured with the Sylvie 3D Drape Tester device equipped with rings that influence draping dynamically. The inner diameter of the applied ring is 210 mm. Measurements were carried out at room temperature. Drape coefficient is calculated with the following conventional relation (6).

$$DC = \frac{A_r - \pi R_1^2}{\pi R_2^2 - \pi R_1^2} \cdot 100 [\%] \quad (6)$$

where DC is the drape coefficient, πR_2^2 is the area of the fabric sample [m^2], A_r is the area of the planar projection of the draping fabric sample [m^2], πR_1^2 is the area of the sample holding table [m^2].

Drape test and its results are shown in Figure 12.



a) b) c)
Figure 12 Draping of sample G163 using a 210 mm diameter ring

a) Top view b) 3D reconstruction and construction lines c) 3D reconstruction

5. Results and discussion

In order to compare the methods of shear angle determination the shear angle values are shown as a function of crosshead movement in Figure 13. In case of the image processing method shear angle was determined at 0 mm, 7.5 mm, 16 mm and 24 mm elongation and crosshead displacement. The diagrams show that the graphs obtained from the results of the own developed method and the geometry based method differ from each other even in their characteristic, while the results of the own developed and the image processing method coincide well, proven by the mean square error (Table 2) as well. Shear angle determined with the image processing method can be considered as authentic since shear angle is measured directly in that case. However, its great disadvantage is that images have to be recorded during the measurement, and these images have to be evaluated and the angles have to be determined manually one by one using image processing software. Besides the need for much manual work, another disadvantage is the subjectivity and the possibility to err during manual evaluation. However, in order to determine the real shear angle image processing is inevitable, otherwise the angle could only be estimated theoretically. Our own developed method works with image processing as well, hence real shear angle can be determined.

Table 2 Shear angle determined with the 3 test methods at 0 mm, 7.5 mm, 16 mm and 24 mm crosshead displacement and the mean square error compared to the results of the image processing method

| Displacement [mm] | | Geometrical | | | | Image processing | | | | Own developed | | | |
|---------------------------------------|--------------------|--------------|--------------|--------------|--------------|------------------|--------|--------|--------|---------------|--------|--------|--------|
| | | G163 | G220 | K170 | C160 | G163 | G220 | K170 | C160 | G163 | G220 | K170 | C160 |
| 0 | Shear angle [°] | 0 | 0 | 0 | 0 | 2.240 | 3.450 | 2.668 | 2.467 | 2.938 | 2.937 | 2.937 | 2.937 |
| | Standard deviation | - | - | - | - | 1.432 | 2.290 | 2.050 | 1.272 | 0.001 | 0.001 | 0.001 | 0.001 |
| 7.5 | Shear angle [°] | 18.765 | 18.765 | 18.765 | 18.765 | 16.728 | 20.284 | 19.063 | 24.530 | 20.705 | 20.441 | 20.494 | 28.323 |
| | Standard deviation | - | - | - | - | 3.028 | 2.664 | 2.951 | 0.042 | 0.969 | 2.371 | 1.098 | 2.542 |
| 16 | Shear angle [°] | 47.253 | 47.253 | 47.253 | 47.253 | 38.540 | 42.424 | 39.300 | 46.545 | 41.485 | 41.237 | 39.290 | 50.575 |
| | Standard deviation | - | - | - | - | 4.196 | 3.636 | 3.316 | 3.939 | 3.155 | 5.695 | 2.605 | 1.772 |
| 24 | Shear angle [°] | cannot calc. | cannot calc. | cannot calc. | cannot calc. | 58.432 | 55 | 54.645 | 63.358 | 57.710 | 51.077 | 49.261 | 60.982 |
| | Standard deviation | - | - | - | - | 5.050 | 2.233 | 3.428 | 3.766 | 3.629 | 2.147 | 3.713 | 1.063 |
| Mean Square Error to image processing | | 4.612 | 3.063 | 4.197 | 3.155 | - | - | - | - | 2.525 | 2.067 | 2.789 | 3.020 |

In case of the geometrical method shear angle is determined based on only the geometrical considerations of longitudinal elongation, for which the measurement itself provides no information at all. Measurement is necessary to be able to calculate shear force from the graph on which tensile force is registered as a function of elongation, and for the calculation of the maximal shear angle maximal elongation is determined. However, the determination of maximal elongation does not always make it possible to determine the maximal shear angle and therefore the shear force, since shear angle can only be calculated until a specific elongation value with this method. The reason is the inverse cosine trigonometric function in formula (3) used for the determination of shear angle, and no number higher than 1 can be the argument of this function. However, the fraction in the argument of this function can already reach 1 far before the end of the measurement, and from then this formula cannot be used. A theoretical shear angle can be determined with the geometrical method and as Figure 13 shows, it differs from the results of the other two methods to a greater and greater extent as crosshead displacement grows.

The diagrams of image processing and the own developed method in Figure 13 do not start from point 0 as the graph of the geometrical method. The reason is that the method based on

geometry always calculates with an initial angle of 90° between the yarns, while the other 2 methods work with the real angles, and the angle between the yarns of the fabric sample is often not exactly 90°.

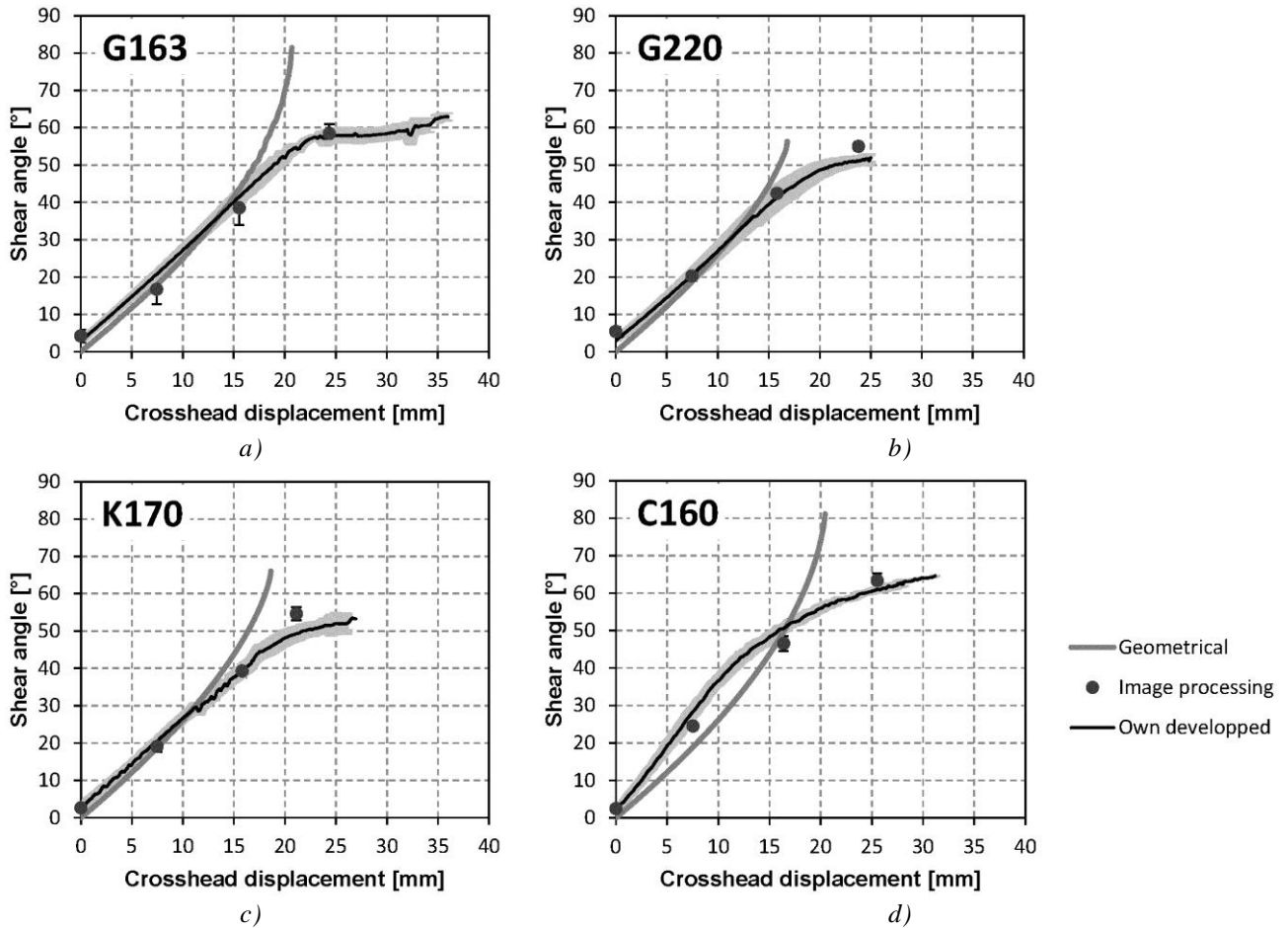


Figure 13 Shear angle-crosshead displacement diagrams with 3 shear angle determination methods
a) Material G163, b) Material G220, c) Material K170, d) Material C160

Shear forces that load the examined fabrics were also calculated using the shear angles determined with our own developed method. Figure 14 illustrates the shear forces as a function of shear angles. There is a significant difference between carbon fabric C160 and the behavior of the other three fabrics. In case of carbon fabric a much higher shear force is needed in order to start shear deformation than in case of the other three samples, and the characteristic of the following parts of the graph also differ to a great extent.

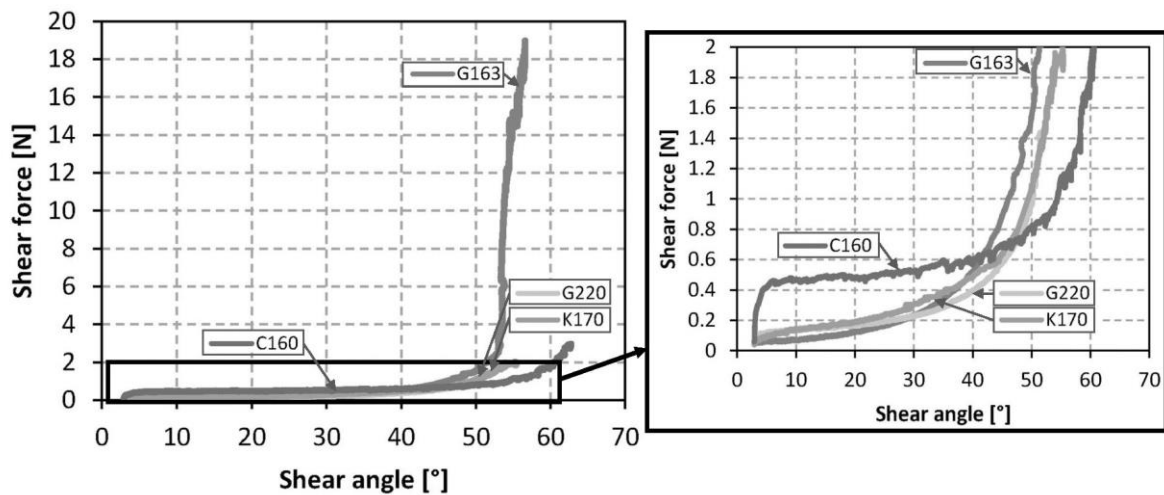


Figure 14 Shear angle – shear force diagrams

Yarn pull-out force characterizes the relation among yarns well. Measurement results are presented in Figure 15 and they reveal that the examined yarn length has impact on the yarn pull-out force, as the yarn pull-out force grows if the number of crossing yarns increases. During the examination the yarn pull-out force increases in the beginning due to the sticking friction among the yarns, and when the yarn passes a crossing yarn the force drops dramatically. If the yarn is pulled further the force increases again but does not reach the previous maximum and later the force drops again when the next crossing yarn is passed. This process repeats itself, and the force maximums decrease as the number of crossing yarns decreases as well, until there are no more crossing yarns and the force reaches zero.

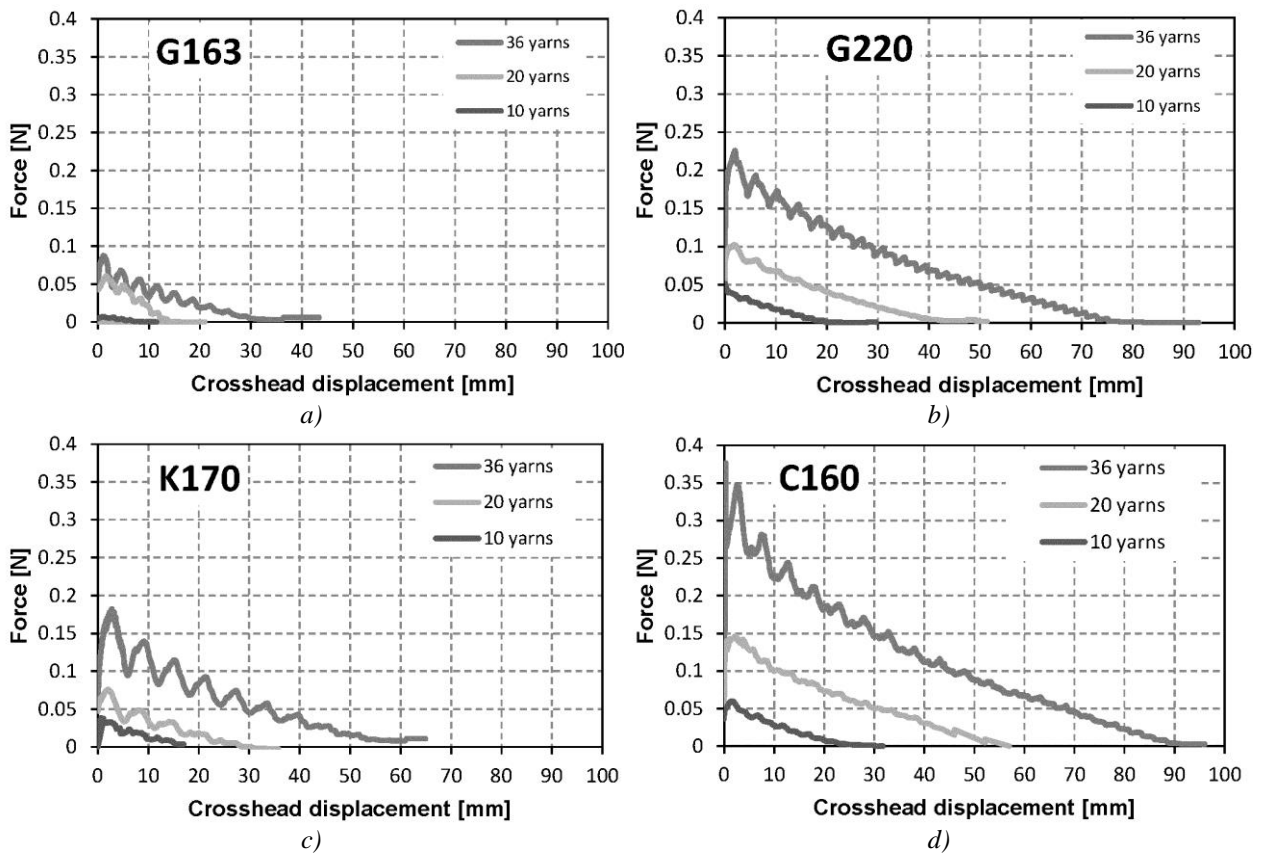
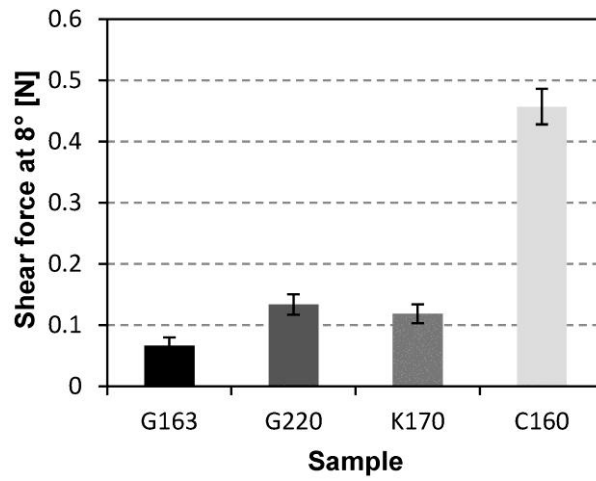


Figure 15 Yarn pull-out force – crosshead displacement curve in case of 10, 20 and 36 crossing yarns

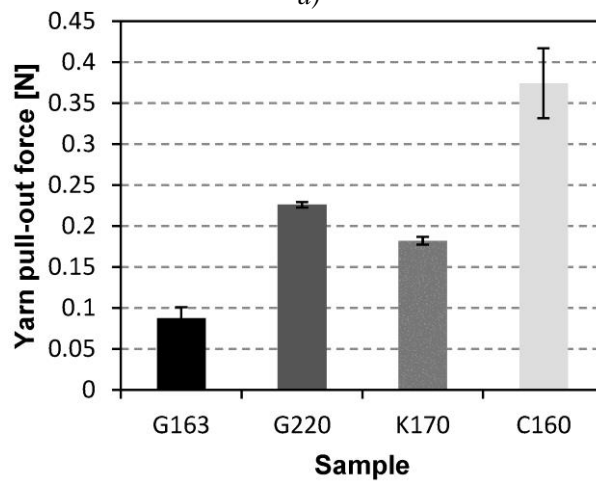
a) Material G163, b) Material G220, c) Material K170, d) Material C160

The maximal yarn pull-out force belonging to the measurement with 36 crossing yarns was chosen in order to characterize the results of the yarn pull-out tests since this value is the most significant. This yarn pull-out force was used for the characterization of the resistance of our examined fabrics against yarn pull-out. Shear force belonging to 8° shear angle was used for the characterization of the shear test results since the conventionally used KES measuring device examines the fabrics until 8° shear angle. This shear force was used for the characterization of the resistance of our examined fabrics against shearing. Results are shown in the diagrams of Figures 16.a and b. In case of the examined fabrics shear force is in strong relation with the yarn pull-out force and as the diagrams show, they change proportionally. This result is up to our expectations, since both characteristics are influenced to the greatest extent by the same friction factor among the yarns.

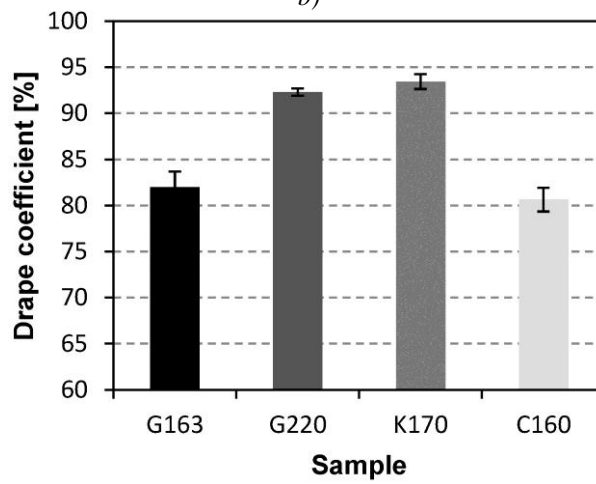
Figure 16 illustrates the results of drape tests. The drape coefficient of fabrics is smaller if the resistance of the fabric against shearing is also smaller and shear force is expected to change simultaneously with the yarn pull-out force in case of conventional drape tests. However, in this research draping was measured with the device equipped with a ring that influences draping dynamically. Therefore the tendency changed. The most significant change can be experienced in case of carbon fabric C160. As it was already mentioned in Chapter 4.3 when describing the measurement, deformation induced by the ring can only get back to the initial shape in an elastic way partly – mainly due to the inhibition effect of the sticking friction among the yarns –, hence the deformation of the sample is larger, and the drape coefficient is smaller than in the case without the ring. That is why in case of using the ring in the measurement increasing shear force – meaning usually an increasing friction coefficient among the yarns – resulted in a smaller drape coefficient, Carbon fabric, for example had the largest shear force, and the smallest drape coefficient as well. This way draping results closer to the application cases were obtained than if the measurement was carried out in the conventional way.



a)



b)



c)

Figure 16 Characteristics of the reinforcing fabrics in case of the 4 samples

a) Shear force at 8° shear angle b) Maximal yarn pull-out force in case of 36 crossing yarns

c) Drap coefficient in case of a 210 mm diameter ring

6. Conclusion

A new measurement method was developed for the determination of the shear angle that is formed during bias extension. The shear angle of fabric reinforcements can be determined more accurately and simply with the new method than earlier, therefore shear force can also be calculated more precisely. Besides shear examination, yarn pull-out tests also characterize the relation among yarns well. Our examinations revealed that these tests show similar tendencies – as expected – since both characterize the relation among yarns, and both are influenced by the friction coefficient among the yarns to the greatest extent. Drapability was measured with a drape tester equipped with a ring that influences drape formation dynamically. Therefore a result opposed to the results of conventional drape measurements was obtained between the drape coefficient and the shear force and the yarn pull-out force. This way results closer to the application cases were obtained than if conventional methods were used. After the analysis of the relation among shear force, yarn pull-out force and drape coefficient it could be concluded that these properties provide adequate information on the formability of reinforcing fabrics if all three are used together.

Acknowledgement

This work is connected to the scientific program of the ‘Development of quality-oriented and harmonized R+D+I strategy and functional model at BME’ project. This project is supported by the New Széchenyi Plan (Project ID: TÁMOP-4.2.1/B-09/1/KMR-2010-0002) and by the Hungarian Scientific Research Fund (OTKA, H), since this study has been carried out as a part of project K68438 (OTKA-NDA).

References

1. J. Wang, J. R. Page, and R. Paton, *Composites Science and Technology*, **58**, 229 (1998).

2. S. B. Sharma, M. P. F. Sutcliffe, and S. H. Chang, *Composites Part A: Applied Science and Manufacturing*, **34**, 1167 (2003).
3. X. Q. Peng, J. Cao, J. Chen, P. Xue, D. S. Lussier, and L. Liu, *Composites Science and Technology*, **64**, 11 (2004).
4. J. Cao, R. Akkerman, P. Boisse, J. Chen, H. S. Cheng, E. F. de Graaf, J. L. Gorczyca, P. Harrison, G. Hivet, J. Launay, W. Lee, L. Liu, S. V. Lomov, A. Long, E. de Luycker, F. Morestin, J. Padvoiskis, X. Q. Peng, J. Sherwood, T. Stoilova, X. M. Tao, I. Verpoest, A. Willems, J. Wiggers, T. X. Yu, and B. Zhu, *Composites Part A: Applied Science and Manufacturing*, **39**, 1037 (2008).
5. J. Rausch, R. C. Zhuang, and E. Mäder, *Express Polymer Letters*, **4**, 576 (2010).
6. D. Bhattacharyya, P. Maitrot, and S. Fakirov, *Express Polymer Letters*, **3**, 525 (2009).
7. G. Czel and T. Czigany, *Plastics Rubber and Composites*, **40**, 369.
8. A. Yang, I. Sul, S. Yoon, S. Kim, and C. Park, *Fibers and Polymers*, **10**, 539 (2009).
9. L. M. Vas and K. Balogh, *Journal of Macromolecular Sciences Part B – Physics*, **B 41**, 977 (2002).
10. P. Tamás, "3D Dress Design (PhD thesis in Hungarian)", Budapest University of Technology and Economics, Budapest, 2008.
11. S. Jevšnik and J. Geršak, *Fibres & Textiles in Eastern Europe* **12**, 47 (2004).
12. S. Jevšnik and D. Žunič-Lojen, *Fibers and Polymers*, **8**, 550 (2007).
13. P. Tamás, J. Geršak, and M. Halász, *Tekstil*, **10**, 497 (2006).
14. N. Pan and M.-Y. Yoon, *Textile Research Journal*, **63**, 629 (1993).
15. Z. Dong and C. T. Sun, *Composites Part A: Applied Science and Manufacturing*, **40**, 1863 (2009).
16. K. Bilisik, *Fibers and Polymers*, **12**, 1106.
17. U. Mohammed, C. Lekakou, L. Dong, and M. G. Bader, *Composites Part A: Applied Science and Manufacturing*, **31**, 299 (2000).

18. P. Potluri, D. A. Perez Ciurezu, and R. B. Ramgulam, *Composites Part A: Applied Science and Manufacturing*, **37**, 303 (2006).
19. J. Domskienė and E. Strazdienė, *Fibres & Textiles in Eastern Europe* **13**, 26 (2005).
20. C. Galliot and R. H. Luchsinger, *Composites Part A: Applied Science and Manufacturing*, **41**, 1743 (2010).
21. S. V. Lomov, P. Boisse, E. Deluycker, F. Morestin, K. Vanclooster, D. Vandepitte, I. Verpoest, and A. Willems, *Composites Part A: Applied Science and Manufacturing*, **39**, 1232 (2008).
22. P. Harrison, M. J. Clifford, and A. C. Long, *Composites Science and Technology*, **64**, 1453 (2004).
23. J. Wiggers, "Analysis of Textile Deformation during Preforming for Liquid Composite Moulding", 2007.
24. W. Lee, J. Padvoiskis, J. Cao, E. De Luycker, P. Boisse, and F. Morestin, *Int J Mater Form*, **1**, 895 (2008).
25. G. Lebrun, M. N. Bureau, and J. Denault, *Composite Structures*, **61**, 341 (2003).
26. T. J. P. I. Federation, "Carbon fibre-Determination of the tensile properties of the single-filament specimens", Japanese Standards Association, Japan, 2000.
27. B. Al-Gaadi, F. Göktepe, and M. Halász, *Textile Research Journal*, **82**, In Press (2012).